ACS OMEGA

http://pubs.acs.org/journal/acsodf

Article

Enhancement of Heat and Mass Transfer in the DCMD Process Using UV-Assisted 1-Hexene-Grafted PP Membranes

Iván Darío Luna-Santander, Rosa María Gómez-Espinosa,* Arturo García-Bórquez, and Beatriz Torrestiana-Sánchez*

Cite This: *ACS Omega* 2022, 7, 44903−44911

Read Online

ACCESS | Metrics & More | Article Recommendations

ABSTRACT: The two main challenges for industrial application of membrane distillation (MD) are mitigation of temperature polarization and reduction of high-energy consumption. Despite the development of advanced materials and the configuration improvements of MD units, membrane surface modification is still one of the alternatives to overcome temperature polarization and improve membrane performance. This work reports a novel and simple method to modify the physical and chemical properties of the polypropylene membrane in order to improve its performance in direct contact membrane distillation (DCMD). The membrane was grafted by polymerization with 1-hexene, UV irradiation, and benzophenone as a photoinitiator. A grafting degree of up to 41% was obtained under UV irradiation for 4 h. The performance of the modified membrane in DCMD was evaluated at different temperatures and salt concentrations in the feed. First, it was found that there was an increase of the vapor permeate flux in the MD process within the range of tested temperatures and salt concentrations. The results were analyzed in terms of the physical properties of the membrane, the transport phenomena, and the thermal efficiency of the process. Theoretical analysis of the results indicated that grafting increased the transfer coefficients of mass and heat of the membrane. Hence, it improved the membrane performance and the thermal efficiency of the DCMD process.

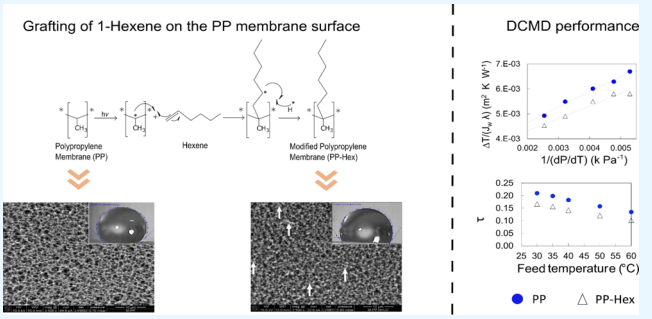

INTRODUCTION

Membrane distillation (MD) is a non-isothermal membrane separation process that separates the liquid phase from the vapor phase of the feed through a hydrophobic microporous membrane. The driving force in MD is the vapor pressure difference across the membrane induced by a temperature gradient between the feed and the permeate solution.[1,2] Hence, MD has several potential applications, such as the production of distilled water (DW) from high-salinity water, the concentration of aqueous solutions, the removal of volatile organic compounds from water, and the separation of non-volatile components, among others.[3−6]

The membrane properties are one of the most important factors for a successful MD process.[7] Currently, membranes are made of hydrophobic polymers such as polypropylene (PP), polyethylene, polyvinylidene fluoride (PVDF), and polytetrafluoroethylene (PTFE).[8] Among these, PP offers additional advantages such as low surface energy, low thermal conductivity, good mechanical properties, and chemical stability.[9−11] Moreover, there is the possibility of modifying the surface properties of the membranes to further improve their performance in the MD process. The UV-induced graft polymerization of a monomer into the polymer matrix is a suitable procedure to modify the membrane wettability or permeability.[9,12] The membrane surface can be modified with different functional groups such as alkene, carboxylic acid, amine, hydroxyl, and sulfonic acid. These groups could be introduced within a polymeric matrix using a blend or immobilization process. 1-Hexene was the choice because it is an excellent candidate to modify the surface properties of PP due to its chemical bonding capacity, nonpolar property, and relatively low cost. Most of the UV photo-grafting research is focused on modifying polymeric membranes with hydrophilic monomers such as acrylic acid, 2-hydroxyethyl methacrylate, 2,4-phenylenediamine, ethylenediamine, cellulose, potato starch, and chitosan.[9,13−17] Modifying membranes with hydrophobic groups includes surface segregation,[18] plasma treatment,[19] covalent modification,[20] electrospinning,[2] and spin coating.[21] To our knowledge, no UV photo-grafting works

Received: August 8, 2022
Accepted: November 17, 2022
Published: December 2, 2022

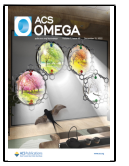

focused on modifying polymeric membranes with 1-hexene have been reported in the literature. Furthermore, most of the research on the chemical grafting of membranes is focused on the effect of the chemical treatment on the physical properties of membranes and their separation properties,[20] and only a few theoretical studies have been reported.[6,22]

Vanneste et al. (2018)[23] adapted a thermal efficiency parameter in the Schofield model to accurately determine the temperature polarization coefficient (TPC) and the thermal conductivity of 17 commercial membranes. Nevertheless, the heat-transfer coefficients of the total boundary layer involved in the MD process were not reported.

Martínez-Diez and Vázquez-González (1999)[24] determined some membrane properties and the heat-transfer coefficient in the boundary layers of two membranes (PTFE and PVDF). Others focused their analysis only on the mass-transfer coefficient (membrane permeability) without considering the heat-transfer phenomena. Efforts have also been made to experimentally analyze the heat and mass transfer in DCMD. Macedonio et al. (2013)[25] used a specifically designed device with temperature sensors located on the membrane surface and the bulk on both the feed and permeate sides. They reported that experimental heat transfer and TPC were in reasonable agreement with their theoretical values when laminar flow is considered and conductive heat flux through the membrane is neglected. The work reported by these authors[20] was also conducted by using a microporous polymeric (PVDF) commercial membrane. Therefore, there is a need to have further insights into the effect of chemical grafting on the membrane's physical properties and its impact on the transport phenomena and thermal efficiency in the MD process of surface-modified membranes.

In this work, a polypropylene membrane was modified by UV-induced graft polymerization with 1-hexene in the presence of a photoinitiator. The unmodified and modified PP membranes were evaluated in the DCMD process by using NaCl aqueous feed solutions and different temperature gradients. The effect of chemical modification was analyzed in terms of membrane microstructure and surface properties, heat and mass transport mechanisms, and thermal efficiency in the DCMD process.

1. Fundamentals of Heat- and Mass-Transfer Phenomena in DCMD. In DCMD, the membrane permeate flux, J_v, is driven by the difference in vapor pressure between the feed and distillate streams at membrane surfaces; in most cases, the models suggest that the mass flux can be written as eq 1[11,27]

$$J_v = C_m(p_{f,m} - p_{p,m}) \tag{1}$$

where C_m is the membrane mass-transfer coefficient, and $p_{f,m}$ and $p_{p,m}$ are the vapor pressures at the membrane surface on the feed side and the permeate side, respectively. The membrane mass-transfer coefficient C_m is a function of the characteristics of the membrane, including thickness, nominal pore size distribution, porosity, and pore tortuosity. As the vapor pressure is not directly measurable, it is convenient to express eq 1 as a function of temperature by linearizing the vapor pressure−temperature dependence[28]

$$J_v = C_m \left.\frac{dp}{dT}\right|_{\bar{T}_m} (T_{f,m} - T_{p,m}) \tag{2}$$

where $T_{f,m}$ and $T_{p,m}$ are the temperatures at the membrane surface of the feed side and the permeate side, respectively. Dp/dT can be evaluated from the extended Antoine equation under the mean temperature of the membrane ($\bar{T}_m$)[29]

$$\left.\frac{dp}{dT}\right|_{\bar{T}_m} = \left(-\frac{C_2}{T_m^{\,2}} + \frac{C_3}{T_m} + C_4 C_5 T_m^{\,C_5-1}\right) e^{(c_1 + c_2/T_m + c_3 \ln T_m + c_4 T_m^{\,C_5})} \tag{3}$$

Where C_1, C_2,C_3,C_4, and C_5 are the extended Antoine equation coefficients and are equal to 73.649, 73.649, −7258.2, 4.1653 × 10^{-6}, and 2, respectively. It should be noted that, for dilute aqueous solutions, vapor pressure is appropriately described by the Antoine equation. For more concentrated aqueous solutions, the vapor pressure needs to be multiplied by a solute-specific expression of the activity coefficient and the molar concentration of the solute.[23,28]

Due to the heat transfer resistance, the temperature at the membrane surface differs from the temperature in the bulk feed (T_f) or permeate (T_p) in the flow channels. The ratio of the temperature differences across the membrane to the bulk temperature difference is defined as the TPC (or τ)[23]

$$\tau = \frac{T_{f,m} - T_{p,m}}{T_f - T_p} \tag{4}$$

When the value of τ approaches unity, it describes a thermally efficient process. Hence, the water vapor flux through the membrane can be calculated based on the bulk temperature difference

$$J_v = C_m \left.\frac{dp}{dT}\right|_{\bar{T}_m} (T_f - T_p)\,\tau \tag{5}$$

By conducting a heat balance over the membrane, an expression for τ can be derived as a function of the different heat-transfer coefficients. The total heat transfer through the membrane (Q_{total}) is equal to the sum of convective and conductive heat transfer

$$Q_{total} = J_v\lambda + \frac{k_m}{\delta}(T_{f,m} - T_{p,m}) \tag{6}$$

where λ is the heat of vaporization of water (slightly dependent on temperature), and k_m and δ are the thermal conductivity and the thickness of the membrane, respectively. Substituting the permeate flux, J_v, from eq 2, yields

$$Q_{total} = \left(C_m \left.\frac{dp}{dT}\right|_{T_m} \lambda + \frac{k_m}{\delta}\right)(T_{f,m} - T_{p,m}) \tag{7}$$

The first factor on the right-hand side of eq 7 constitutes the total membrane heat-transfer coefficient (H)

$$H = C_m \left.\frac{dp}{dT}\right|_{\bar{T}_m} \lambda + \frac{k_m}{\delta} = q_v + q_c \tag{8}$$

where q_v is the heat transfer due to the vapor flowing through the membrane, and q_c is the heat transfer by conduction in the membrane. In the stationary state, the total heat transfer through the membrane equals total heat transfer through the boundary layer on either side of the membrane

$$Q_{total} = h_f(T_f - T_{f,m}) = h_p(T_{p,m} - T_p) \tag{9}$$

https://doi.org/10.1021/acsomega.2c05075
ACS Omega 2022, 7, 44903−44911

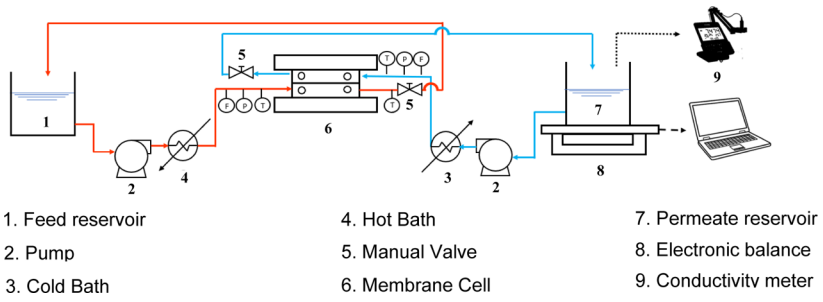

Figure 1. Experimental setup for the DCMD system.

where h_f and h_p are the convective heat-transfer coefficients of the feed and permeate boundary layers, respectively. Combining eqs 4 and 7−9 yields an expression for the TPC (τ) as a function of different heat-transfer coefficients

$$\tau = \frac{1}{\left(1 + \frac{H}{h_f} + \frac{H}{h_p}\right)} \tag{10}$$

In DCMD operated with dilute solutions, the hydrodynamics on the feed and permeates are very similar when the same cross-flow velocity, channel geometry, and spacers are used. The convective heat-transfer coefficients of the feed and distillate boundary layers are therefore similar to those of the plate-and-frame modules and can be lumped together in a total boundary layer heat-transfer coefficient (h)

$$h = \frac{1}{\left(\frac{1}{h_f} + \frac{1}{h_p}\right)} \tag{11}$$

Substituting eqs 10 and 11 into eq 5 yields an expression that clearly illustrates the strong coupling between mass- (C_m) and heat-transfer (H, h) coefficients in MD

$$J_v = C_m \left.\frac{dp}{dT}\right|_{\bar{T}_m} (T_f - T_p) \frac{1}{\left(1 + \frac{H}{h}\right)} \tag{12}$$

Substituting eq 8 in eq 12 and rearranging gives

$$\frac{\Delta T}{J_v \lambda} = \frac{1}{dp/dT} \frac{1}{C_m \lambda}\left(1 + \frac{k_m/\delta}{h}\right) + \frac{1}{h} \tag{13}$$

where ΔT is the difference between T_f and T_p. Equation 13 is the Schofield model, and it may be used for the analysis of experimental results, where T_f, T_p, and J_v are reported. Since dp/dT is a function of $T_m = (T_f - T_p)/2$, it can be assumed that the temperature polarization is similar on both sides of the membrane. Provided that k_m and δ can be estimated or measured, the only unknown parameters in eq 13 are h and C_m, which can be obtained from the intercept and slope, respectively, by plotting $\Delta T(J_v\lambda)^{-1}$ versus $(dp/dT)^{-1}$ from eq 13 for different temperatures.

A parameter closely related to thermal conductivity is the thermal efficiency (η) of the membrane. η is the fractional contribution of vapor transport to the overall energy transfer across the membrane. Therefore, the classical definition of thermal efficiency incorporates the thermal conductivity[23,30]

$$\eta = \frac{q_v}{Q_{total}} = \frac{J_v \lambda}{J_v \lambda + \frac{k_m}{\delta}(T_{f,m} - T_{p,m})} \tag{14}$$

A low value of η indicates significant heat conduction loss through the membrane, and values approaching 1 are desirable.

2. MATERIALS AND METHODS

2.1. Materials. The materials used in this work include a flat polypropylene membrane (3M) with 0.0073 m^2 surface area (A), 0.45 μm pore size, 114 μm thickness, and 84.6% porosity; 1-hexene (97%, Sigma-Aldrich); benzophenone (98.5%, Sigma-Aldrich); acetone (99.5%, J.T.Baker); and sodium chloride ACS reagent (Sigma-Aldrich).

2.2. Experimental Setup and Process Conditions. The DCMD module was equipped with a single pristine or modified PP membrane. The feeds tested were 3.5 and 5 wt % sodium chloride (NaCl) aqueous solutions. The temperature of the feed and permeate solutions at the inlet of the membrane module was maintained constant by using heat exchangers (Figure 1).

Pressure <5 psi on both sides of the membrane was constantly monitored by pressure sensors located at the feed and permeate inputs and outputs of the module. The initial volume of the feed and permeate solutions was 1 L. The flow rates of feed and permeate solutions were 0.1 L min^{-1}. It has been reported that partial pore wetting might occur, and this will decrease salt rejection and flux during the process.[30] To evaluate if pore wetting occurs during the process, permeate solution conductivity was measured in every run using a conductivity meter (Thermo Scientific Orion Star A215).

The conductivity of the permeate solution at the beginning and the end of each experiment was registered. The process performance in terms of the vapor permeate flow rate was followed by the weight gain at the permeate reservoir by using a precision balance attached to a computer (Figure 1). The run time was 12 h for both the original and modified PP membranes under all tested conditions. Permeate flux (J_v) was calculated from the collected data by using the following equation[31]

$$J_v = \frac{W_2 - W_1}{(t_2 - t_1) \times A} \tag{15}$$

where A is the surface area of the membrane, and W_2 and W_1 are the permeate weights at times t_2 and t_1, respectively.

The salt rejection (R) can be calculated by

$$R = 1 - \frac{C_p}{C_f} \tag{16}$$

$$C_p = \frac{C_2 V_2 - C_1 V_1}{V_2 - V_1} \tag{17}$$

https://doi.org/10.1021/acsomega.2c05075
ACS Omega 2022, 7, 44903−44911

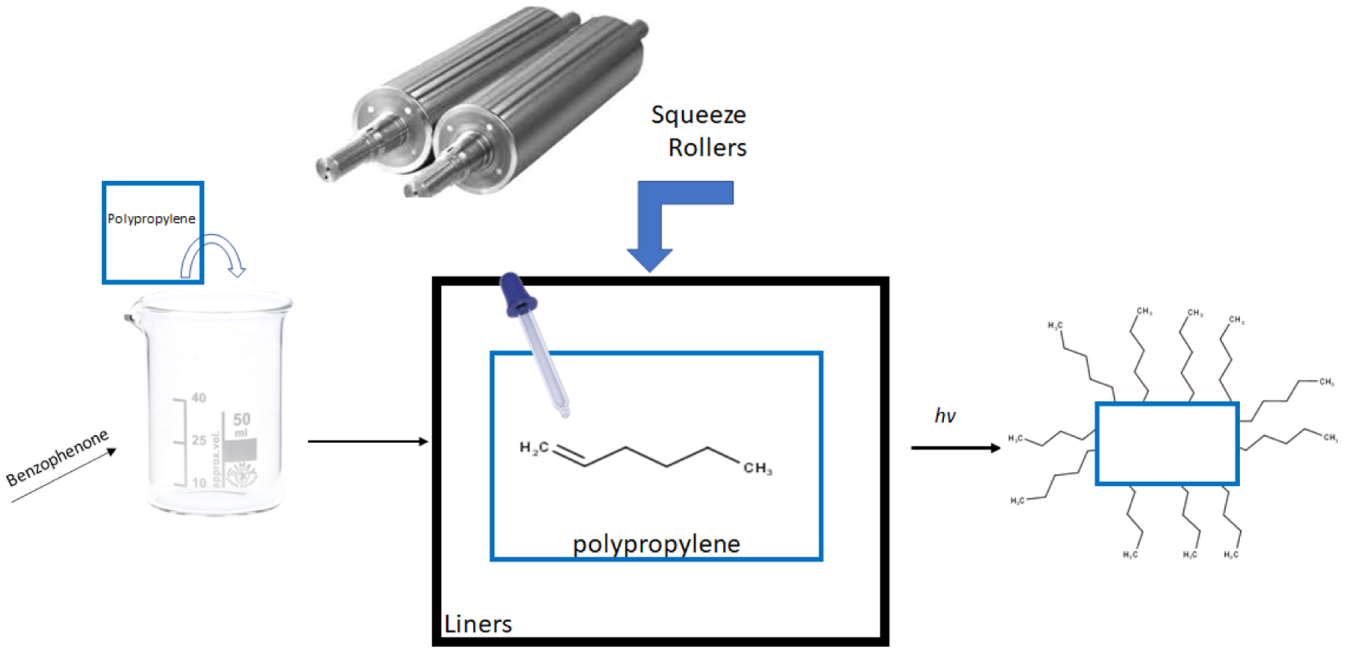

Figure 2. Detailed graphics of the membrane modification process.

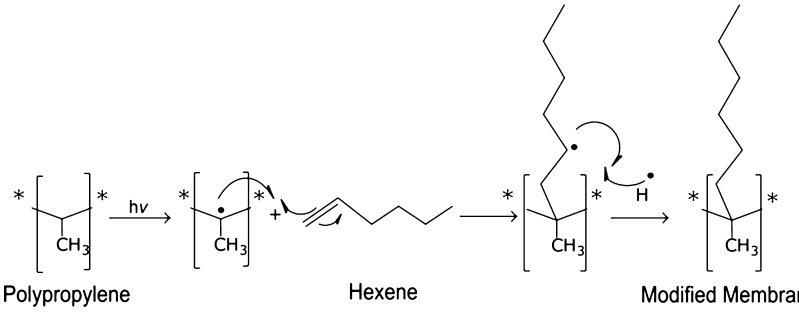

Figure 3. Proposal for a grafting mechanism of 1-hexene on the PP surface assisted by UV irradiation.

where C_p (wt %) is the permeate salt concentration, and C_f (wt %) is the salt concentration of the feed solution. C_1 and C_2 are the salt concentrations, and V_1 and V_2 are the volumes of liquid in the permeate reservoir measured at times t_1 and t_2, respectively. The salt concentration of the permeate solution was obtained from a conductivity versus salt concentration standard curve.[32]

2.3. Chemical Modification of the Membrane. A two-step chemical treatment was carried out to modify the properties of the PP membrane. In the first step, membranes were immersed in a benzophenone solution (5 wt % in acetone) for 5 min and dried at room temperature. In the second step, the PP membranes were immersed into a 97% 1-hexene solution between two liners placed in squeeze rollers (Figure 2) and transferred to a glass plate under UV irradiation for 2, 4, and 6 h. Thereafter, the membranes were separated from the glass plate, immersed in ketone to remove the residual monomer, and dried in a desiccator for 12 h at room temperature.

The degree of 1-hexene grafted (% D_g) was calculated from the equation

$$\%D_g = \frac{W_1 - W_0}{W_0} X100 \quad (18)$$

where W_0 and W_1 are the weights of the unmodified and grafted PP membranes, respectively. By measuring this gain in weight, the amount of the grafted monomer can be determined.

2.4. Membrane Characterization. The membranes were characterized before and after the grafting process by scanning electron microscopy (SEM), attenuated total reflectance-Fourier transform infrared (ATR-FTIR) spectroscopy, and contact angle measurement. These techniques provide information on morphological changes, the presence of surface molecular groups, and hydrophobicity, respectively.

2.4.1. FTIR Spectroscopy. FTIR spectroscopy was used for the qualitative analysis of the functional groups on the membrane surface to verify if surface modification had occurred. The spectra were acquired using an infrared spectrometer, PerkinElmer ATR-FTIR; the spectrum acquisition conditions were 25 °C, 64 scans between 500 and 4000, and 1 cm^{-1} spectral resolution.

2.4.2. Low-Vacuum Scanning Electron Microscopy. Membrane microstructure analysis was carried out by using an FEI, low-vacuum scanning electron microscopy (LV-SEM) Quanta 3D FEG, to determine if chemical treatment induced morphological changes in grafted membranes. To avoid thermal deformation and accumulation of electric charge in the samples, they were previously covered with an ultra-thin

https://doi.org/10.1021/acsomega.2c05075
ACS Omega 2022, 7, 44903−44911

Au film, and a low vacuum of 0.6−0.7 mbar was generated in the SEM sample chamber during the observations.

2.4.3. Cavity Size Estimation. As cavity is considered the gap that remains between polymer chains, the cross-sectional area was considered as a measure of its size for comparison purposes. The measurements were made one by one manually to avoid ambiguities in the extension of the cavity, which was measured in length and width. Once the average cross-sectional area of the cavities was determined, an equivalent diameter was calculated, considering a circle with the said area.

2.4.4. Water Contact Angle. The water contact angle was obtained using the sessile drop method with a Ramé-Hart Inc. system, model 100/07/00. The drop images were stored and analyzed by drop-analysis with Image-J (Image processing and analysis in Java software). Average values of the advancing angle were obtained after six measurements made at 20 °C using 10 mL of purified water.

3. RESULTS AND DISCUSSION

3.1. Graft Polymerization Reaction. The first step is to generate a free radical on tri-substituted carbon atoms in the PP carbon chain, which can react with the carbon−carbon double bond of 1-hexene, producing a bond between the membrane and the 1-hexene monomer (Figure 3).

The ATR-FTIR spectra provide information about functional groups at the membrane surface. Figure 4 shows the ATR-FTIR spectra of the unmodified and modified PP membranes at different UV-irradiation times; calculated grafting degrees are also indicated for each treatment time. The ATR-FTIR spectrum of the unmodified membrane shows typical signals of polypropylene, according to the literature,[9,12] specifically at 2919 and 2840 cm^{-1} for the asymmetric and symmetric stretching vibrations of CH_2, respectively, while, at 1449 and 1376 cm^{-1} for the scissor vibrations of CH_2. Furthermore, the weak absorption peaks at 1170, 990, 970, and 840 cm^{-1} are in good agreement with those reported by Prabowo et al. (2016),[33] with the first vibration corresponding to the C−C bending and the others appearing in isotactic PP.

When comparing the ATR-FTIR spectrum of the unmodified PP membrane with the spectra of the UV-irradiated membranes, no differences were observed, except at the spectrum of the UV-irradiated membrane for 4 h, which shows two additional absorption peaks at 1648 and 699 cm^{-1}, corresponding to a double bond C═C and a low frequency −C−C− stretching vibration, respectively. Such signals prove that 1-hexene monomer was successfully grafted onto the PP membrane surface after 4 h of UV-irradiation, in good agreement with the highest grafting degree of 41% calculated for this modified PP membrane. By using the 2 h UV-irradiated PP membrane, only 10% grafting degree is obtained, the expected extra signals being too weak (perhaps two times lower than the 4 h-modified membrane) to be detected. In contrast, after 6 h, UV-irradiation results in 0% ($w_0 = w_1$, at eq 18) of grafting degree and no extra FTIR signals, suggesting polypropylene degradation, that is, a balance between the gain (monomer) and loss (PP) of weight. Furthermore, the lower intensities of the main absorption bands in the 6 h-modified membrane spectrum, compared to those of the pristine membrane, reinforce the idea of loss of membrane by degradation. These experimental facts point out an important result to be taken into account: polypropylene is susceptible to suffering degradation under long-term UV irradiation.

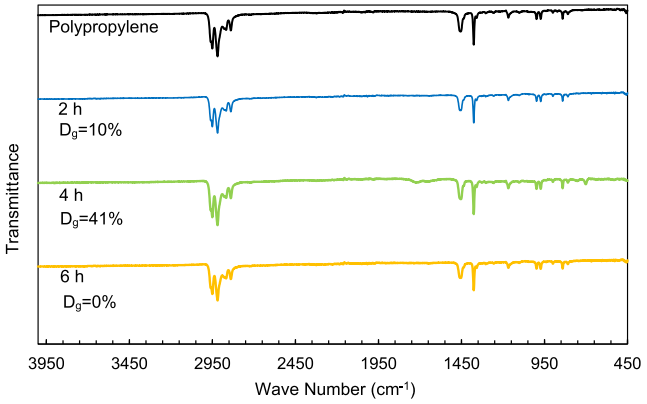

Figure 4. ATR-FTIR spectra of the unmodified and modified PP membranes at different UV-irradiation times: 2, 4, and 6 h. Calculated grafting degrees (D_g) from eq 18 are also indicated for each treatment time.

3.2. Morphological and Surface Properties. Figure 5 shows images of the SEM and contact angles of the unmodified (left) and 4 h-UV chemically modified (right) membranes. Static CA was measured on both sides of the modified and unmodified membranes, and the resulting values are compared in Table 1. As can be seen, CA changes only substantially after grafting and only on the front surface, that is, the feed side. To elucidate this behavior, SEM images were taken before and after the grafting process.

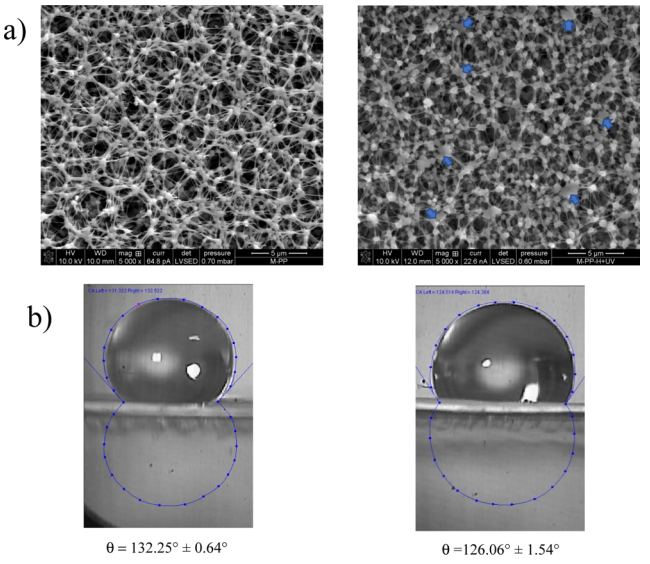

Figure 5. Images of (a) SEM and (b) contact angles (θ) unmodified (left) and modified (right) PP membranes. Such experimental evidence reinforces the ATR-FTIR interpretation of the 1-hexene monomer grafted into the PP membrane.

Table 1. Comparison of the Static Contact Angles on Both Sides of the Membranes for Unmodified and Modified Membranes

samples	M-PP	M-PP-H + UV
front surface	132.25 ± 0.6	126.0 ± 1.5
back surface	126.7 ± 0.4	126.97 ± 0.87

https://doi.org/10.1021/acsomega.2c05075
ACS Omega 2022, 7, 44903−44911

In the SEM image of Figure 5a-left, it is observed that the polymeric chains on the surface of the original membrane form a mesh of rings with diameters of the order of micrometers, namely 1.16 μm as the equivalent diameter, corresponding to an average cavity cross-sectional area of 1.05 μm^2. On the other hand, in the SEM image of Figure 5a right of the surface of the PP membrane treated for 4 h, it is observed that this arrangement of rings deteriorates and the membrane itself becomes denser, which is reflected in an increase in the contact area, corresponding to a decrease in the average cavity cross-sectional area, namely 0.168 μm^2, or an equivalent diameter of 0.46 μm. It must be taken into account that these estimates correspond exclusively to the surface of the membrane. Experimentally, this change is detected by a slight decrease in the static contact angle without the membrane no longer being classified as hydrophobic since it generates a contact angle greater than 90°, specifically 126.06° against 132.25° in the original membrane, barely a variation of 5%. In image 5a-right, extra features are also observed in the form of thin flakes, some of them indicated by arrows, which have been associated with the insertion of the 1-hexane monomer.

It is known that hydrophobicity is influenced both by a chemical component, in our case, the presence of 1-hexane, and by a physical component, surface tension, which is usually measured by the static contact angle on a homogeneous and smooth surface, which is far from being our case as we have more holes than solid matter on the surface (Wenzel regime). On this last point, there are controversies in the literature regarding the effectiveness of the contact angle as a measure of hydrophobicity; for example, Law (214)[34] proposes the measurement of two angles, one at the exact moment when the drop of water makes contact with the surface (advancing angle) and the other when detaching from it (receding angle), which are related with the wetting and adhesion forces, respectively. For our purposes, we will only say that the measured contact angle is not able to perceive the influence of the chemical part, that is, the presence of 1-hexane, since its density on the surface is low, predominating the physical part, that is, the increase in the contact area as the polymeric rings partially fade in the grafted membrane, perhaps under the influence of UV radiation. However, the presence of 1-hexane in the volume of the grafted membrane, as can be seen in the SEM image in the cross-section in Figure 6, decisively contributes to the rejection of liquid water and favors the flow of steam, as will be discussed later.

3.3. Effect of Grafting on Membrane Performance (Salt Rejection and Vapor Flux). The water vapor flux of the pristine and modified PP membranes was compared in the DCMD process under different salinities and feed temperatures. No significant variations in NaCl rejection (97.6 ± 0.42%) were observed between the virgin and modified PP membranes under all tested conditions. Figure 7 shows the permeate flux and retentate conductivity profiles obtained with both virgin and modified PP membranes for one of the conducted experimental runs.

It also shows that 1-hexene, grafted by UV polymerization, increased the vapor flux of the modified PP membrane by more than 10%.This effect was observed for both distilled water (DW) and NaCl aqueous solutions, see Figure 8.

This figure also shows that the feed temperature between 40 and 60 °C increased the vapor permeate flux (J_v) in both membranes by about threefold. More specifically, the permeate flux increased by 4 kg per square meter per hour for every 10 degree centigrade increase at the feed temperature between 40 and 60°. This result is due to the rise in vapor pressure produced in the temperature range tested, according to the Antoine equation.[24−35] Otherwise, J_v decreased slightly but systematically with increments in the salt concentration in both membranes, indicating that the vapor transport through the pores is more hampered as the feed salinity increases. Although, the salinity concentration range tested was limited (0, 3.5, and 5 wt %), the trend agrees with that reported in the literature,[36,37] where it was found that the permeate flux is significantly affected up to relatively high NaCl concentrations (17.76 and 24.68 wt %). The performance of the modified PP membrane during DCMD obtained in this work with 3.5 wt % NaCl is in the range of that reported in the literature for membranes modified by using sophisticated methods.[10,18−20] The vapor permeate flux and permeate conductivity profiles obtained with both virgin and modified PP membranes obtained for this solution (3.5 wt % NaCl) are shown in Figure 8.

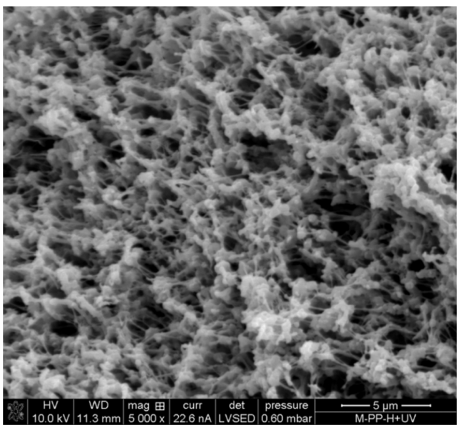

Figure 6. Cross-sectional SEM image of the membrane grafted for 4 h.

3.4. Effect of Grafting on Transport Properties. Experimental data from both membranes were compared in terms of Schofield's model (Equation 13). The convective heat-transfer coefficient, h, and the membrane mass-transfer coefficient, C_m, obtained from the intercept and the slope of graphs from Figure 8, respectively, are shown in Table 2. It can be seen that the UV-grafting of 1-hexene increased the mass-transfer coefficient, C_m, in the modified PP membrane compared to the unmodified one by 21.6%. This result is aligned with the positive effect of grafting on the water vapor flux of the modified membrane (Figure 9).

A 15.2% increment was also seen in the heat-transfer coefficient, H, of the UV-irradiated and chemically modified PP membrane compared to the H value of the unmodified one. This effect on H might be the result of the increased mass of vapor transferred through the membrane (q_v) during the DCMD process. Phattaranawik et al. (2003)[38] demonstrated that the q_v effect in the heat transfer varied from 46 to 62% in PVDF membranes and up to 92% in PP membranes.[11] Hence, q_v is the main component of heat transfer inside the membrane.[11,39] A slight increase in the convective heat-transfer coefficient, h, was also determined for the modified membrane. This suggests a slightly higher thermal resistance in the boundary layer, probably due to a slightly higher concentration of salt ions at the surface of the modified membrane.

https://doi.org/10.1021/acsomega.2c05075
ACS Omega 2022, 7, 44903−44911

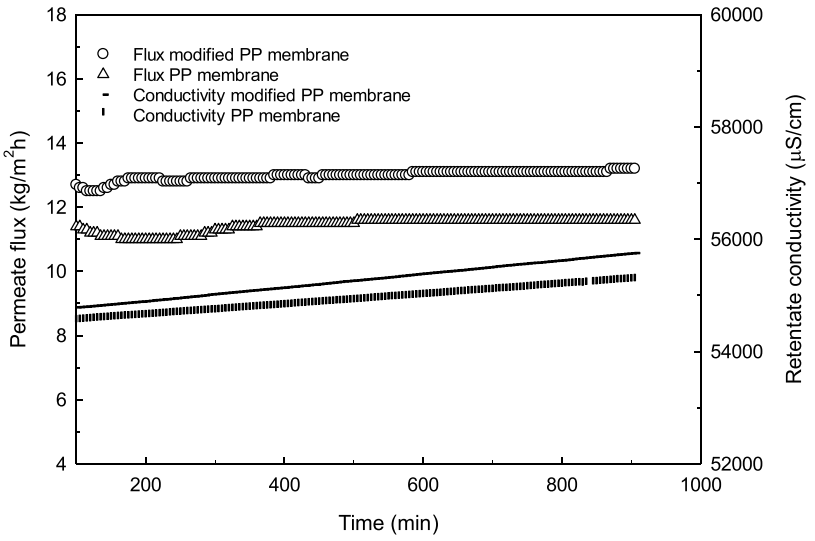

Figure 7. Vapor permeate flux and retentate conductivity for the DCMD of 3.5% NaCl solutions obtained with the virgin and modified PP membranes under the following conditions: feed temperature: 60 °C, permeate temperature: 20 °C, feed and permeate flow rates: 0.1 $Lmin^{-1}$.

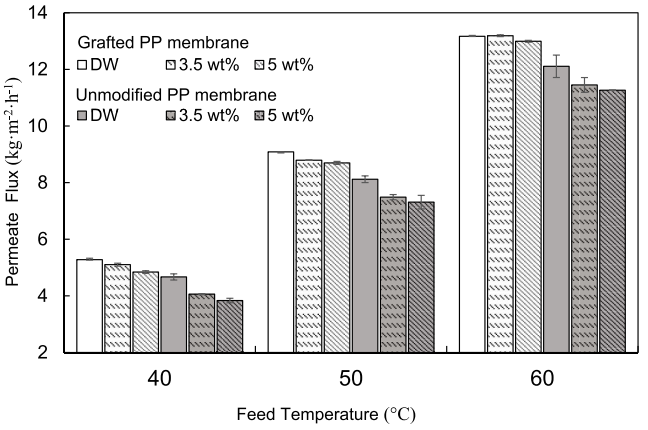

Figure 8. Permeate flux of the unmodified and grafted PP membranes was obtained at different temperatures and NaCl concentrations (0, 3.5, and 5 wt %) in the feed solution. Permeate temperature was kept constant at 20 °C, along with feed and permeate flow rates at 0.1 $Lmin^{-1}$.

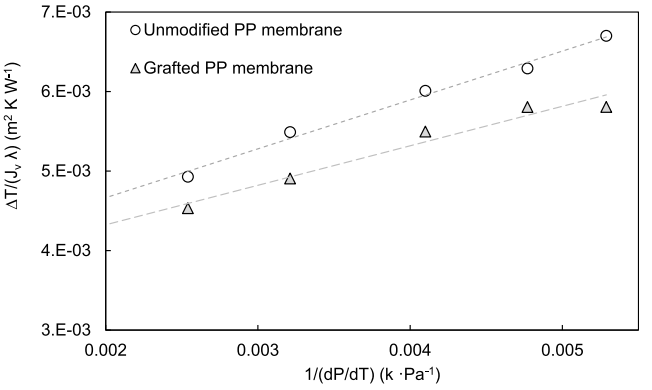

Figure 9. Prediction of the heat- and mass-transfer coefficients of modified and unmodified PP membranes by using the Schofield model (eq 13).

Table 2. Effect of Grafting on the Transport Properties of PP Membranes according to the Schofield Model at 40 °C

coefficient	unmodified PP membrane	modified PP membrane
C_m 10^7(kg m^{-2} s^{-1} Pa^{-1})	15.5	18.8
H(W m^{-2} K^{-1})	1302.7	1500.9
h(W m^{-2} K^{-1})	291.1	300.6

The effect of the feed temperature on the TPC (τ) was also analyzed. Figure 10 shows that τ decreases when increasing the feed temperature for both membranes. The rise in the feed temperature increased the rate of heat transport from the feed to the membrane permeate side, and this decreased the temperature at the feed membrane boundary layer. The result of the increased transport of heat via convection and conduction through the membrane combined with the cooling effect caused by evaporation at the feed side on the membrane surface appears as a decrease in the TPC.[40] Therefore, results

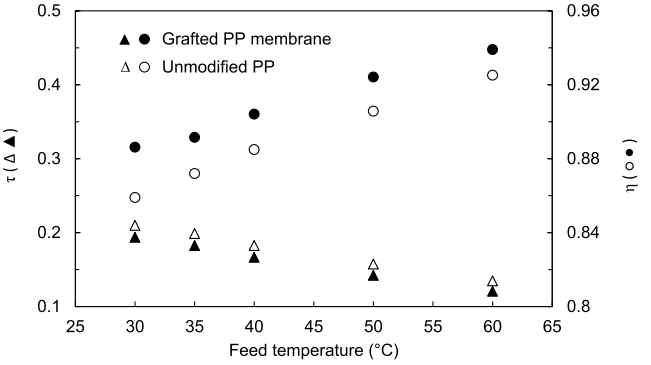

Figure 10. Temperature polarization coefficient (τ) and thermal efficiency (η) as a function of the feed temperature on the DCMD process with the unmodified and modified PP membranes by using DW as feed. Permeate inlet temperature: 20 °C, feed and permeate flow rates: 0.1 L/min.

indicate that the energy consumption required for water evaporation at the membrane surface increased at higher temperatures.[11,24,41]

https://doi.org/10.1021/acsomega.2c05075
ACS Omega 2022, 7, 44903−44911

Figure 10 also shows that τ of the modified membrane is lower than that of the unmodified one in the whole range of temperatures tested. This might be the consequence of a larger mass of vapor evaporated at the feed of the modified membrane surface, which demanded higher energy consumption. Despite this, results analyzed in terms of the thermal efficiency (η) of the DCMD process with both unmodified and modified membranes show that η increased by raising the feed temperature.

The improvement in the thermal efficiency was smaller as the temperature of the feed stream increased; that is, at the feed temperature of 30 °C, a 3% increase in τ was obtained, while at the feed temperature of 60 °C, the increase of η was 1.5%. The thermal efficiency of the process with the modified membrane was higher in the whole range of feed temperatures tested. This effect points out that grafting favored the transfer of heat through the membrane; hence, the MD process with the modified membrane will consume less energy than the MD process with the unmodified membrane.

4. CONCLUSIONS

A hydrophobic membrane was obtained by grafting 1-hexene onto the polypropylene membrane surface with the assistance of UV radiation and a photoinitiator. FT-IR and SEM confirmed the successful grafting of 1-hexene on the membrane surface. Changes in the microstructure of the grafted membrane surface were followed by SEM images showing a decrease in the average cross-sectional area of the membrane from 1.05 to 0.168 μm^2 or in the equivalent diameter from 1.16 to 0.46 μm. These changes resulted in a 5 % reduction of the contact angle. Despite that, the insertion of 1-hexene molecules in the whole membrane microstructure increased the vapor permeate flux in the MD process at all tested temperatures and salt concentrations. Salinity decreased the permeate flux J_v under all temperature conditions in both modified and unmodified membranes. This effect was lower in the modified membranes than in the unmodified ones. The theoretical analysis of the results by using the Schofield model and the contribution of vapor transport to the overall energy transfer across the membrane suggests that the insertion of 1-hexene molecules in the modified PP membrane increased the mass and heat transfer and improved the thermal efficiency of the DCMD process.

AUTHOR INFORMATION

Corresponding Authors

Rosa María Gómez-Espinosa − *Centro Conjunto de Investigación en Química Sustentable, UAEM-UNAM, Universidad Autónoma del Estado de México, Toluca 50200, Mexico*; Email: rmgomeze@uamex.com

Beatriz Torrestiana-Sánchez − *Tecnológico Nacional de México/IT-Veracruz, Veracruz, Ver. 91897, Mexico*; orcid.org/0000-0001-8295-1608; Email: beatriz.ts@tecnm.veracruz.mx

Authors

Iván Darío Luna-Santander − *Tecnológico Nacional de México/IT-Veracruz, Veracruz, Ver. 91897, Mexico*

Arturo García-Bórquez − *Instituto Politécnico Nacional, ESFM, Ciudad de México 07320, Mexico*

Complete contact information is available at: https://pubs.acs.org/10.1021/acsomega.2c05075

Notes

The authors declare no competing financial interest.

ACKNOWLEDGMENTS

The authors thank the Mexican National Council of Science and Technology (CONACyT) for the scholarship granted to I. D. Luna-Santander during his graduate studies. The authors also thank M. Sc. Salvador Lopez Morales from the Materials Research Institute of the National University of Mexico (IIM-UNAM) for his technical assistance in the determination of the membranes' water contact angle, as well as Dra. Mayahuel Ortega Avilés from the Center for Nanosciences and Micro- and Nanotechnologies of the National Polytechnic Institute (IPN) for her invaluable support with the low-vacuum SEM. One of the authors, AGB, thanks the financial support through the IPN research project SIP20221575.

ABBREVIATIONS

A	membrane surface area, m^2
$c_{i;i=1,2,3,4,5}$	extended Antoine equation coefficients
C_m	membrane mass-transfer coefficient, kg m^{-2} Pa^{-1} s^{-1}
C	salt concentration, kg_{salt} kg_{water}^{-1}
CA	contact angle
D_g	grafting degree, %
H	membrane heat-transfer coefficient, W m^{-2}
h	convective heat-transfer coefficient, W m^{-2}
J_v	vapor permeate flux, kg m^{-2} s^{-1}
k	conductivity, W m^{-1} K^{-1}
p	vapor pressure, Pa
t	time, s
T	temperature, K
$\overline{T}$	mean temperature, K
Q	heat transfer through the boundary layer, W m^{-2}
q	heat transfer through the membrane, W m^{-2}
V	volume, m^3
W	weight, kg
τ	temperature polarization coefficient, [-]
δ	membrane thickness, m
λ	heat of vaporization, W m^{-2}

SUBSCRIPTS

v	vapor
m	membrane
f	feed
p	permeate
f,m	feed membrane side
p,m	permeate membrane side
c	conduction
Δ	gradient

REFERENCES

(1) Anari, Z.; Sengupta, A.; Sardari, K.; Wickramasinghe, S. R. Surface modification of PVDF membranes for treating produced waters by direct contact membrane distillation. *Sep. Purif. Technol.* **2019**, *224*, 388−396.

(2) Liao, Y.; Wang, R.; Fane, A. G. Engineering superhydrophobic surface on poly(vinylidene fluoride) nanofiber membranes for direct contact membrane distillation. *J. Memb. Sci.* **2013**, *440*, 77−87.

(3) G, G.; G, G.; Af, I. Perspective of renewable desalination by using membrane distillation. *Chem. Eng. Res. Des.* **2019**, *144*, 520−537.

(4) Kadi, K.; Hashaikeh, R.; Ahmed, R.; Janajreh, I. Design and performance evaluation of a portable hybrid desalination unit using direct contact membrane distillation in dual configuration. *Energy Procedia* **2019**, *158*, 904−910.
(5) Cong, S.; Liu, X.; Guo, F. Membrane distillation using surface modified multi-layer porous ceramics. *Int. J. Heat Mass Transf.* **2019**, *129*, 764−772.
(6) Manawi, Y. M.; Khraisheh, M.; Fard, A. K.; Benyahia, F.; Adham, S. Effect of operational parameters on distillate flux in direct contact membrane distillation (DCMD): Comparison between experimental and model predicted performance. *Desalination* **2014**, *336*, 110−120.
(7) Xu, Z.; Liu, Z.; Song, P.; Xiao, C. Fabrication of super-hydrophobic polypropylene hollow fiber membrane and its application in membrane distillation. *Desalination* **2017**, *414*, 10−17.
(8) Drioli, E.; Ali, A.; Macedonio, F. Membrane distillation: Recent developments and perspectives. *Desalination* **2015**, *356*, 56−84.
(9) Hernández-Aguirre, O. A.; Núñez-Pineda, A.; Tapia-Tapia, M.; Espinosa, R. M. G. Surface Modification of Polypropylene Membrane Using Biopolymers with Potential Applications for Metal Ion Removal. *J. Chem.* **2016**, *2016*, 1−11.
(10) Korolkov, I. V.; Gorin, Y. G.; Yeszhanov, A. B.; Kozlovskiy, A. L.; Zdorovets, M. V. Preparation of PET track-etched membranes for membrane distillation by photo-induced graft polymerization. *Mater. Chem. Phys.* **2018**, *205*, 55−63.
(11) Phattaranawik, J.; Jiraratananon, R.; Fane, A. G. Heat transport and membrane distillation coefficients in direct contact membrane distillation. *J. Memb. Sci.* **2003**, *212*, 177−193.
(12) Hollman, A. M.; Bhattacharyya, D.*Chapter 16 Functionalized membranes for tunable separations and toxic metal capture*; Elsevier Masson SAS, 2003.
(13) Palacios-Jaimes, M. L.; Cortes-Guzman, F.; González-Martínez, D. A.; Gómez-Espinosa, R. M. Surface modification of polypropylene membrane by acrylate epoxidized soybean oil to be used in water treatment. *J. Appl. Polym. Sci.* **2012**, *124*, E147−E153.
(14) Rahimpour, A.; Madaeni, S. S.; Zereshki, S.; Mansourpanah, Y. Preparation and characterization of modified nano-porous PVDF membrane with high antifouling property using UV photo-grafting. *Appl. Surf. Sci.* **2009**, *255*, 7455−7461.
(15) Majidi Salehi, S.; Di Profio, G.; Fontananova, E.; Nicoletta, F. P.; Curcio, E.; De Filpo, G. Membrane distillation by novel hydrogel composite membranes. *J. Memb. Sci.* **2016**, *504*, 220−229.
(16) Figoli, A.; Ursino, C.; Galiano, F.; Di Nicolò, E.; Campanelli, P.; Carnevale, M. C.; Criscuoli, A. Innovative hydrophobic coating of perfluoropolyether (PFPE) on commercial hydrophilic membranes for DCMD application. *J. Memb. Sci.* **2017**, *522*, 192−201.
(17) Stragliotto, M. F.; Strumia, M. C.; Gomez, C. G.; Romero, M. R. Optimization of UV-Induced Graft Polymerization of Acrylic Acid on Polypropylene Films Using CdS as Light Sensor. *Ind. Eng. Chem. Res.* **2018**, *57*, 1188−1196.
(18) Khayet, M.; Essalhi, M.; Qtaishat, M. R.; Matsuura, T. Robust surface modified polyetherimide hollow fiber membrane for long-term desalination by membrane distillation. *Desalination* **2019**, *466*, 107−117.
(19) Yang, X.; Wang, R.; Shi, L.; Fane, A. G.; Debowski, M. Performance improvement of PVDF hollow fiber-based membrane distillation process. *J. Memb. Sci.* **2011**, *369*, 437−447.
(20) Amirilargani, M.; Merlet, R. B.; Nijmeijer, A.; Winnubst, L.; de Smet, L. C. P. M.; Sudhölter, E. J. R. Poly (maleic anhydride-alt-1-alkenes) directly grafted to γ-alumina for high-performance organic solvent nanofiltration membranes. *J. Memb. Sci.* **2018**, *564*, 259−266.
(21) Jung, J.; Shin, Y.; Choi, Y. J.; Sohn, J.; Lee, S.; An, K. Hydrophobic surface modification of membrane distillation (MD) membranes using water-repelling polymer based on urethane rubber. *Desalin. Water Treat.* **2016**, *57*, 10031−10041.
(22) Wang, P.; Chung, T. S. Recent advances in membrane distillation processes: Membrane development, configuration design and application exploring. *J. Memb. Sci.* **2015**, *474*, 39−56.
(23) Vanneste, J.; Bush, J. A.; Hickenbottom, K. L.; Marks, C. A.; Jassby, D.; Turchi, C. S.; Cath, T. Y. Novel thermal efficiency-based model for determination of thermal conductivity of membrane distillation membranes. *J. Memb. Sci.* **2018**, *548*, 298−308.
(24) Martínez-Díez, L.; Vázquez-González, M. I.; Florido-Díaz, F. J. Temperature polarization coefficients in membrane distillation. *Sep. Sci. Technol.* **1999**, *33*, 787−799.
(25) Macedonio, F.; Ali, A.; Poerio, T.; El-Sayed, E.; Drioli, E.; Abdel-Jawad, M. Direct contact membrane distillation for treatment of oilfield produced water. *Sep. Purif. Technol.* **2014**, *126*, 69−81.
(26) Eykens, L.; Hitsov, I.; De Sitter, K.; Dotremont, C.; Pinoy, L.; Nopens, I.; Van der Bruggen, B. Influence of membrane thickness and process conditions on direct contact membrane distillation at different salinities. *J. Memb. Sci.* **2016**, *498*, 353−364.
(27) Khayet, M. Membranes and theoretical modeling of membrane distillation: A review. *Adv. Colloid Interface Sci.* **2011**, *164*, 56−88.
(28) Schofield, R. W.; Fane, A. G.; Fell, C. J. D. Heat and mass transfer in membrane distillation. *J. Memb. Sci.* **1987**, *33*, 299−313.
(29) Perry, R. H., Green, D. W., Maloney, J. O.*Perry's Chemical Engineers' Handbook*, 7th ed.; McGraw-Hill Education, 1997.
(30) Rezaei, M.; Warsinger, D. M.; Lienhard V, J. H.; Duke, M. C.; Matsuura, T.; Samhaber, W. M.*Wetting Phenomena in Membrane Distillation: Mechanisms, Reversal, and Prevention*; Elsevier B.V., 2018.
(31) Hou, D.; Wang, J.; Sun, X.; Luan, Z.; Zhao, C.; Ren, X. Boron removal from aqueous solution by direct contact membrane distillation. *J. Hazard. Mater.* **2010**, *177*, 613−619.
(32) Ho, C. D.; Chang, H.; Chang, C. L.; Huang, C. H. Theoretical and experimental studies of flux enhancement with roughened surface in direct contact membrane distillation desalination. *J. Memb. Sci.* **2013**, *433*, 160−166.
(33) Prabowo, I.; Nur Pratama, J.; Chalid, M. The effect of modified ijuk fibers to crystallinity of polypropylene composite. *Mats. Sci. Eng.* **2017**, *223*, 012020.
(34) Law, K.-Y. Definitions for Hydrophilicity, Hydrophobicity, and Superhydrophobicity: Getting the Basics Right. *Phys. Chem. Lett.* **2014**, *5*, 686−688.
(35) Gryta, M. The study of performance of polyethylene chlorinetrifluoroethylene membranes used for brine desalination by membrane distillation. *Desalination* **2016**, *398*, 52−63.
(36) Alkhudhiri, A.; Darwish, N.; Hilal, N. Membrane distillation: A comprehensive review. *Desalination* **2012**, *287*, 2−18.
(37) Susanto, H. Towards practical implementations of membrane distillation. *Chem. Eng. Process.* **2011**, *50*, 139−150.
(38) Phattaranawik, J.; Jiraratananon, R. Direct contact membrane distillation: Effect of mass transfer on heat transfer. *J. Memb. Sci.* **2001**, *188*, 137−143.
(39) Yun, Y.; Ma, R.; Zhang, W.; Fane, A. G.; Li, J. Direct contact membrane distillation mechanism for high concentration NaCl solutions. *Desalination* **2006**, *188*, 251−262.
(40) Fadhil, S.; Marino, T.; Makki, H. F.; Alsalhy, Q. F.; Blefari, S.; Macedonio, F.; Nicolò, E.; Giorno, L.; Drioli, E.; Figoli, A. Novel PVDF-HFP flat sheet membranes prepared by triethyl phosphate (TEP) solvent for direct contact membrane distillation. *Chem. Eng. Process.* **2016**, *102*, 16−26.
(41) Ho, C. D.; Chang, H.; Chang, C. L.; Huang, C. H. Theoretical and experimental studies of flux enhancement with roughened surface in direct contact membrane distillation desalination. *J. Memb. Sci.* **2013**, *433*, 160−166.

https://doi.org/10.1021/acsomega.2c05075
ACS Omega 2022, 7, 44903−44911